Postprint

Aerobic Homocoupling of Arylboronic Acids Catalyzed by Regenerable Pd(II)@MIL-88B-NH$_2$(Cr)

Alejandro Valiente,[a] Sergio Carrasco,[a] Amparo Sanz-Marco,[a] Cheuk-Wai Tai,[c] Antonio Bermejo Gómez,[a,b] and Belén Martín-Matute*,[a]

Abstract: A fast and operationally simple method for the aerobic homocoupling of arylboronic acids is described. The process is catalyzed by Pd(II) complexes supported on the metal-organic framework MIL-88B-NH$_2$(Cr). The benefits of this approach include the use of a benign oxidant / solvent mixture at room temperature with catalytic amounts of base, easy recovery of the catalyst, and easy isolation of the products. Very high conversions and good yields were achieved for a variety of substrates, and the process was also carried out on a larger scale with the same efficiency. The catalyst was found to suffer deactivation due to progressive reduction and agglomeration of palladium into inactive metal clusters/particles. An innovative procedure for the oxidative redispersion and regeneration of the active Pd(II)@MOF species is presented.

Introduction

In recent years, the transition-metal-mediated aerobic oxidation of organic substrates has become an area of increasing interest for the chemical community.[1] The need for efficient oxidation processes that are compatible with the idea of sustainable chemistry is hugely important, and this must be addressed through the development of methods involving benign oxidants, green solvents, and recyclable catalysts.[2] Heterogeneous Pd-catalyzed protocols based on the use of molecular oxygen now represent a highly promising and versatile approach to achieving this goal. Examples of dehydrogenation reactions[3] or Wacker processes,[4] of C–H functionalization[5] and of C–C bond formation[6] through heterogeneous Pd-catalyzed aerobic oxidation have recently been reported. Representative examples of the latter type of reaction include the oxidative coupling of carbon nucleophiles such as arylboronic acids to obtain biaryls,[7] or the Glaser-Hay reaction to synthesize diynes.[8]

The oxidative homocoupling of arylboronic acids was first reported by Davidson and coworkers in 1968 using stoichiometric amounts of palladium.[9] However, it was not until 1996 that Moreno-Mañas and coworkers reported the first catalytic oxidative homocoupling of boronic acids, using palladium complexes with monodentate phosphine ligands.[10] After that, several protocols for catalytic oxidative homocoupling using homogeneous palladium complexes were reported.[11] To the best of our knowledge, there are only three reports of the

use of heterogeneous palladium catalysts for this reaction. The first one was reported in 2006 by Yamamoto and coworkers, who reported the aerobic homocoupling of arylboronic acids in the absence of a base, mediated by Pd(OAc)$_2$ encapsulated in a polyurea matrix (Scheme 1a).[12] In 2016, Li, Wei and coworkers reported a protocol for the oxidative homocoupling of boronic acids and their derivatives using Pd(0) supported on Al(OH)$_3$, with Ag$_2$O as the oxidant and 1 equiv. of base (Scheme 1b).[13] Finally, Kapdi and coworkers described an aerobic procedure for the same reaction based on the use of active palladium colloids and 2 equiv. of base at high temperatures (Scheme 1c).[6]

Scheme 1. Heterogeneous Pd-catalyzed homocoupling of boronic acids.
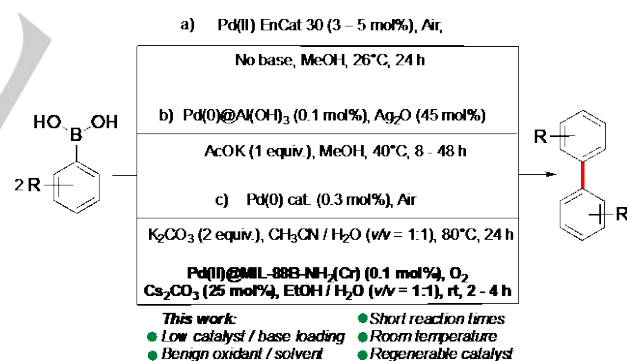
Metal-organic frameworks (MOFs) are currently some of the most widely studied materials,[14] and heterogeneous catalysts based on these materials have become increasingly popular in the last two decades.[15] MOFs are crystalline polymers made up of metallic nodes linked by polytopic organic linkers through strong coordination bonds.[16] They can act as catalysts as synthesized,[17] since the presence of Lewis acid / base sites at metal nodes or linker substituents respectively are reported to promote a wide variety of reactions.[18,19] They are also widely used as supports for other catalysts,[20] such as single-site transition-metal complexes or metal nanoparticles (NPs).[21]

[a] A. Valiente, Dr. S. Carrasco, Dr. A. Sanz-Marco, Dr. A. Bermejo Gómez and Prof. Dr. B. Martín-Matute
Department of Organic Chemistry
Stockholm University
The Arrhenius Laboratory 16C, SE-106 91, Stockholm (Sweden)
e-mail: belen.martin.matute@su.se
[b] Dr. A. Bermejo Gómez
Sprint Bioscience
Hälsovägen 7, SE-141 57, Huddinge (Sweden)
[c] Dr. C.-W. Tai
Department of Materials and Environmental Chemistry
Stockholm University
The Arrhenius Laboratory 16C, SE-106 91, Stockholm (Sweden)

Our group has developed several procedures using Pd nanoparticles supported on MIL-101-NH$_2$(Cr) and MIL-88B-NH$_2$(Cr). The excellent catalytic activity of the resulting materials has been demonstrated in a wide variety of transformations, including Suzuki-Miyaura cross-couplings,[22] C−H activation / halogenations,[23] selective C=C hydrogenations,[24] Heck couplings,[25] different carbonylation reactions[26] and the aerobic oxidation of benzylic alcohols.[27] The catalytic methods we developed using these heterogeneous Pd catalysts were efficient, and in some cases they even surpassed their homogeneous counterparts. Some of the reasons for this high efficiency include the outstanding performance shown by the catalysts under continuous-flow conditions,[22b,27] the successful recycling of the catalyst,[22a,24,27] and the mild reaction conditions used for the reactions.[22,24,26]
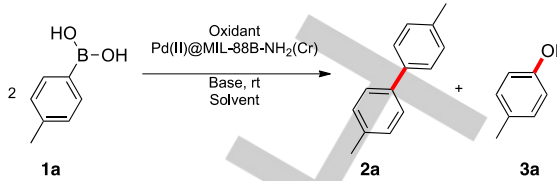
In this paper, we describe an efficient Pd(II)-catalyzed heterogeneous protocol for the fast aerobic homocoupling of arylboronic acids. Pd(II)@MIL-88B-NH$_2$(Cr) was chosen as the catalyst due to its previous good results in terms of activity, stability, and ease of synthesis.[23,26,27] This method showed a high substrate tolerance, and gave good product yields at low catalyst / base loadings under very mild reaction conditions. Further, we present an innovative procedure to regenerate the active catalyst based on the oxidative redispersion of inactive Pd(0) particles at room temperature.

Results and Discussion.

1. Reaction optimization. In 2013, our group reported an efficient procedure for the Suzuki-Miyaura cross-coupling reaction catalyzed by palladium NPs supported on MIL-101-NH$_2$(Cr). The reaction proceeded at room temperature, using 2 equiv. of Cs$_2$CO$_3$ as the base in a mixed solvent of EtOH / H$_2$O (1:1).[22] Interestingly, when *p*-tolylboronic acid (**1a**) was subjected to similar reaction conditions in the absence of the aryl halide and using Pd(II)@MIL-88B-NH$_2$(Cr) (0.4 mol% Pd), a 44% yield of the homocoupled product (**2a**) was obtained (Table 1, entry 1) together with 5% of *p*-cresol (**3a**). When the same reaction was carried out under an oxygen atmosphere, full conversion was observed within 1 h, and a 72% yield of biaryl **2a** was obtained (entry 2). Other oxidants were screened (see ESI, Table S2), but oxygen outperformed the other oxidants tested as it was more efficient and convenient. When the reaction was carried out under argon, no product formation was observed (entry 3).

Concerning the solvent, the effect of the EtOH / H$_2$O ratio was investigated. When pure ethanol or pure water was used, 53 and 50% yields of **2a** were obtained, respectively (entries 4 and 5). When 3:1 or 1:3 (*v/v*) mixtures were used, no improvement in the product yield was observed (43 and 48% respectively; entries 6, 7). Therefore, we continued to use EtOH / H$_2$O 1:1 (*v/v*) as the solvent mixture; under these conditions the desired product **2a** was formed in a higher yield after only 1 h. The catalyst loading was also examined. We found that a catalyst loading of 0.1 mol% gave a similar yield (69% of **2a**; entry 8, TON = 909), increasing the reaction time to 2 h.

Table 1. Optimization of the reaction conditions.[a]

Entry	Cat. (mol %)	Solvent (*v/v*)	Base (equiv.)	Conv (%)	% Yield **2a**[d] / **3a**[f]
1[b]	0.4	EtOH / H$_2$O (1:1)	Cs$_2$CO$_3$ (1)	67	44 / 5
2	0.4	EtOH / H$_2$O (1:1)	Cs$_2$CO$_3$ (1)	>99	72 / 21
3[c]	0.4	EtOH / H$_2$O (1:1)	Cs$_2$CO$_3$ (1)	-	- / -
4	0.4	EtOH	Cs$_2$CO$_3$ (1)	91	53 / 10
5	0.4	H$_2$O	Cs$_2$CO$_3$ (1)	97	50 / 13
6	0.4	EtOH / H$_2$O (3:1)	Cs$_2$CO$_3$ (1)	>99	43 / 13
7	0.4	EtOH / H$_2$O (1:3)	Cs$_2$CO$_3$ (1)	>99	48 / 22
8[e]	0.1	EtOH / H$_2$O (1:1)	Cs$_2$CO$_3$ (1)	>99	69 / 24
10[e]	**0.1**	**EtOH / H$_2$O (1:1)**	**Cs$_2$CO$_3$ (0.25)**	**>99**	**71 / 22**
11[e]	0.1	EtOH / H$_2$O (1:1)	-	-	Traces / -
12[e]	0.1	EtOH / H$_2$O (1:1)	K$_2$CO$_3$ (0.25)	>99	52 / 18
13[e]	0.1	EtOH / H$_2$O (1:1)	KF (0.25)	95	47 / 21
14[e]	0.1	EtOH / H$_2$O (1:1)	KOAc (0.25)	93	43 / 20
15[e]	0.1	EtOH / H$_2$O (1:1)	K$_3$PO$_4$ (0.25)	83	13 / 11

[a] Unless otherwise noted: **1a** (2 mmol), cat.: Pd(II)@MIL-88B-NH$_2$(Cr), 9.22 wt% Pd, O$_2$ (1 atm), rt, 1 h. [b] Under air. [c] Oxidant-free conditions; under an argon atmosphere. [d] Isolated yields. [e] 2 h. [f] Yields determined against an internal standard by ^{1}H NMR spectroscopy; volatile product.

Although some base-free homocoupling protocols are known,[10,11b,12] the need for stoichiometric / excess base is common in this reaction.[11] Interestingly, under our reaction conditions, when the amount of Cs$_2$CO$_3$ was lowered from 100 to 25 mol%, full conversion and a 71% yield of **2a** were obtained after 2 h at room temperature (entry 10). In the absence of base, though, only traces of product were detected (entry 11). When 25 mol% of other bases were used, no improvement in the reaction outcome was observed (entries 12 - 15). Thus, Cs$_2$CO$_3$ showed the best performance of all the bases tested (see ESI Section 3 for further info.).

The crystallinity of the catalyst was analyzed by *ex-situ* X-Ray Powder Diffraction (XRPD), which showed that after being subjected to optimal conditions (entry 10) the structure of the framework remained unaltered (see ESI, Figure S3).

2. Substrate scope and limitations. A variety of substrates were screened under the optimized conditions (Table 1, entry 10) to test the generality of the method (Scheme 2). We first investigated the homocoupling of *para*-substituted phenylboronic acids bearing electron-donating groups (EDG) (**2a-2f**). Good to excellent yields (67 - 91%) were obtained within reasonably short reaction times (2 - 3 h) with the exception of diamine **2e** (21%). It is noteworthy that the method tolerates free benzylic alcohols; product **2d** was obtained in good yield without further oxidation. Additionally, trimethylsilyl substituted arylboronic acid **1f** could be selectively coupled through the C–B [28] bond delivering biaryl **2f** in high yield (81%). Unsubstituted biphenyl **2g** was synthesized in 78% yield after 2 h. Arylboronic halides were tolerated, and compounds **2h** and **2i** were formed in 71 and 65% yields, respectively. Reaction at the chloride group in **2i** was not observed. We then proceeded with substrates bearing electron-withdrawing groups at the *para* position. Aldehyde, nitrile, trifluoromethyl, and ester functionalities were tolerated, and **2j-2m** were formed in good yields (52 - 66%) after 2 - 4 h. *Meta*-substituted substrates bearing EDG delivered biaryls **2n** and **2o** in 72 and 64% yields, respectively. Polysubstituted and polyaromatic arylboronic acids were satisfactorily tolerated, and compounds **2p-2u** were formed in

good to excellent yields (57 - 98%). Remarkably, most of the products were isolated by filtration with no need of additional purification steps; the elemental analysis of **2a** showed that the product isolated in this manner was of very high purity (See ESI, S5).

3. Large-scale reactions. To prove that the efficiency of the method is retained when the reaction is run on gram scale, 41 mmol (5.7 g) of *p*-tolylboronic acid was subjected to the reaction conditions. In this experiment, the amount of base was further lowered to 12 mol% (1.66 g, 5 mmol, ESI, Figure S4). After 2 h at room temperature, 2.5 g (70%) of biaryl **2a** was isolated after a simple filtration (Scheme 3).
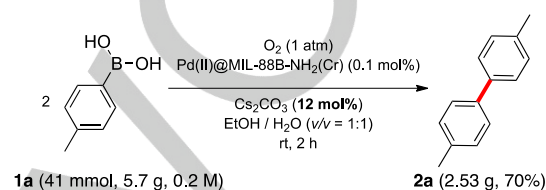
Scheme 3. Large-scale homocoupling of *p*–tolylboronic acid.
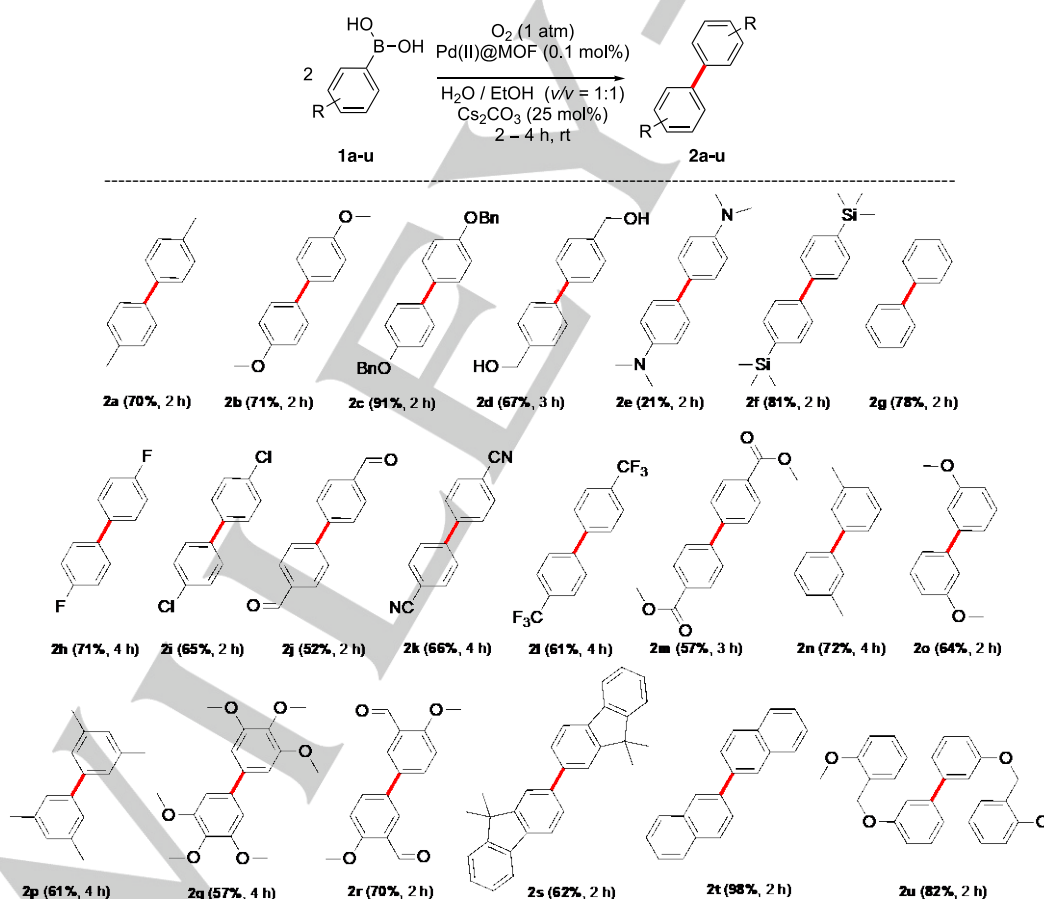
Scheme 2. Aerobic homocoupling of boronic acids. Reaction conditions: **1a-u** (2 mmol), 9.22 wt% Pd(II)@MIL-88B-NH$_2$(Cr) (0.1 mol%), O$_2$ (1 atm), EtOH / H$_2$O (0.2 M, *v/v* = 1:1), Cs$_2$CO$_3$ (25 mol%), rt, 2 - 4 h. Isolated yields.

4. Catalyst recycling and regeneration. The recyclability of Pd(II)@MIL-88B-NH$_2$(Cr) was investigated in the homocoupling of *p*-tolylboronic acid over five consecutive runs. The experiments were carried out at 4 mmol scale. Interestingly, the XRPD pattern of the recovered material revealed that the framework did not decompose after five reaction runs (Figure 1a), despite the previously reported detrimental effect of carbonates on its mesoporous polymorph MIL-101-NH$_2$.[22c] Slight changes were observed in the 2Θ value and relative intensities of the main diffraction peaks; this has been reported previously for this MOF, and ascribed to its flexible nature.[27,29] On the other hand, the activity of the catalyst was retained only until the second run, when a yield of 70% of the main product

a)

b)

Figure 1. a) XRPD patterns of the fresh material (dark blue) and recovered material after runs 1 (green) and 5 (orange). b) Recycling experiments on a 4 mmol scale. Isolated yields (left axis, blue bars) and Pd / Cr ratio in the recovered catalyst after runs 2 and 5 (right axis, orange bars) are represented.

was obtained (Figure 1b, blue bars). Further runs showed a drastic decrease in the catalytic activity, from 30% in run 3 to 7% in run 5. The elemental analysis by ICP-OES (Inductively Coupled Plasma Optical Emission Spectrometry) showed that the Pd/Cr ratio decreased from 0.63 (fresh catalyst, run 0) to 0.48 in the recovered material after 2 runs (Figure 1b, orange bars). However, analysis of the catalyst recovered after run 5 ruled out catalyst leaching as the reason for the dramatic decrease in activity, since the Pd/Cr ratio was 0.47, essentially the same as after run 2.

The *in-situ* reduction of supported palladium complexes to form Pd(0) nanoparticles and their agglomeration are a common cause of catalyst deactivation.[30] Indeed, the analysis by scanning transmission electron microscopy (STEM) of the recovered catalyst after 1 run (Figure 2, a) showed the formation of homogeneously dispersed Pd NPs of 2.6 nm average size (see ESI, Figure S12) within and on the surface of the MOF matrix. After the second cycle (Figure 2, b; see also ESI Figure S8), bigger NPs were found (4.9 nm average size). After the 5th run (Figure 2, c), the particle distribution turned into big surficial agglomerates of Pd (44 nm average size) with partial crystalline character (See ESI, Figure S5), coexisting with some remaining smaller particles. As XRPD data showed (Figure 1a), the STEM images in Figure 2 supported a correct preservation of the MIL-88B-NH$_2$ morphology at the end of the process.

In a control experiment where a Pd(0) surrogate catalyst, Pd(0)@MIL-101-NH$_2$,[31] of well-defined crystalline NPs[32] (see ESI, Figures S7, S10) was used under the optimized reaction conditions, only 15% of **2a** (see ESI, Table S3, entry 14) was isolated after 2 h (compared to 71% using Pd(II)@MIL-88B-NH$_2$; Table 1, entry 10). We believe that the difference in behaviour between these two catalysts is not only due to particle size effects, but to the presence of Pd(II) species. Presumably, when Pd(II) is reduced *in-situ*, the initially formed atomic Pd(0) centers or small Pd(0) clusters react with the reagents before further aggregation occurs, forming bigger Pd(0) nanoparticles, which have a diminished activity.[30,33] Similar observations have been reported by Domingos and coworkers, who reported that only the palladium(II) oxide species found on the surface of Pd nanocubes act as the active catalytic species, whilst the Pd(0) atoms in the nanocubes are unable to enter into the catalytic cycle. [34]
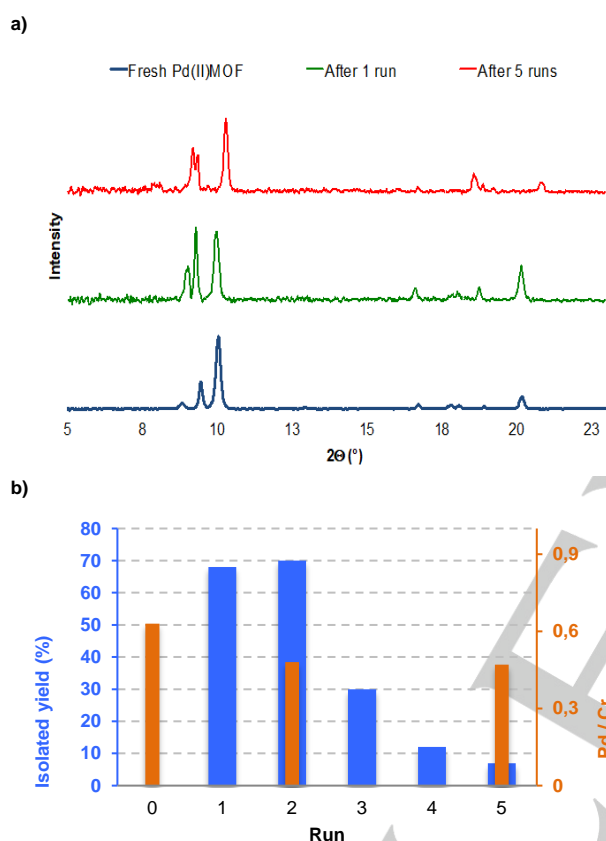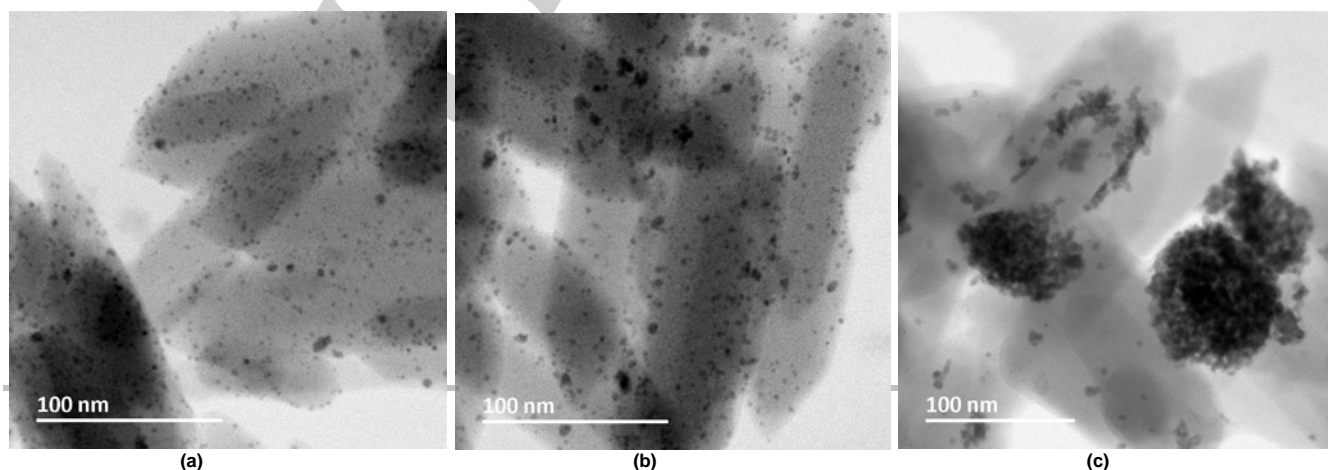

Figure 2. BF-STEM (bright-field STEM) images of the recovered Pd@MIL-88B-NH$_2$ catalysts after runs 1, 2, and 5 (a, b, and c respectively).

For the oxidative coupling reported here, it is therefore plausible that the reduction and aggregation of Pd(0) atoms / clusters into large particles is the main deactivation pathway. To overcome this problem, we envisioned the possibility of restoring the activity of the catalyst by oxidation of the inactive Pd(0) particles. The "redispersion" of metal particles by oxidation / reduction cycles is a known approach for the reactivation of sintered Pd(0) catalysts.[35] There are examples in the literature where oxidants such as nitric acid were used to regenerate sulfide- or carbon-fouled Pd catalysts.[36] However, procedures where oxidants are used to promote the oxidation and redispersion of Pd nanoparticles are rather scarce and commonly performed in very harsh conditions and involving toxic reagents.[37] Further, no example has been reported with MOFs as the support of the metal particles. In 2014, Datye and coworkers described the regeneration of atomically dispersed Pd(II)@Al(OH)$_3$ by high-temperature calcination (700 °C) in air.[38] Due to the harsh conditions, this method does not become suitable for organic-based or hybrid materials (such as MOFs) and / or those having lower thermal stability. In this case the calcination temperature needed is higher than the thermal decomposition of Pd(II)@MIL-88B-NH$_2$(Cr) (T$_d$: 325 °C, see ESI Section 2).[39] For this reason, we aimed to develop a procedure whereby Pd particles could be oxidized and redispersed in the MOF using an oxidant under mild reaction conditions.

Various oxidants were *ex-situ* screened on Pd(0)@MIL-101-NH$_2$ composite, and the resulting materials were subsequently tested for catalytic activity (see ESI, Table S3). We found that upon treatment with potassium peroxodisulfate (K$_2$S$_2$O$_8$, 5 equiv. with respect to Pd) in 2 M HCl, the activity of the oxidized Pd@MIL-101-NH$_2$ emulated that of fresh Pd(II)@MIL-88B-NH$_2$ and, importantly, it did not affect the MOF structure. STEM and XRPD analysis confirmed a successful dispersion of the initial NPs into small nanoclusters, keeping intact the morphology of the support (see ESI, Figures S7, S11).

We then tried to apply the catalyst activation for the homocoupling reaction (runs 1'- 6'; Figure 3b, green bars) under the conditions presented in this manuscript. Thus, after two new runs (1' and 2'), the deactivated recovered catalyst was subjected to the oxidative procedure (Figure 3, Ox$_1$), and a 71 % yield of **2a** was obtained in run 3' (Figure 3b), *vs* 30% obtained in run 3 (blue bar, Figure 3b). Interestingly, the reactivated catalyst kept the same efficiency for an additional run (69% yield in run 4' *vs* 12% in run 4), after which it again showed a decrease in activity (38% in run 5'). To test whether the method could be repeated, the deactivated catalyst from run 5' was again subjected to oxidative treatment (Figure 3, Ox$_2$). Gratifyingly, the catalyst recovered its original activity once again, and a yield of 71% of **2a** product was obtained in a sixth run (6').

The STEM analysis of the catalyst obtained after two oxidative treatments (Ox$_2$) showed that the number of Pd(0) clusters was dramatically reduced (Figure 4 *vs* Figure 2; see also ESI Figures S8 and S9), and that the morphology of the
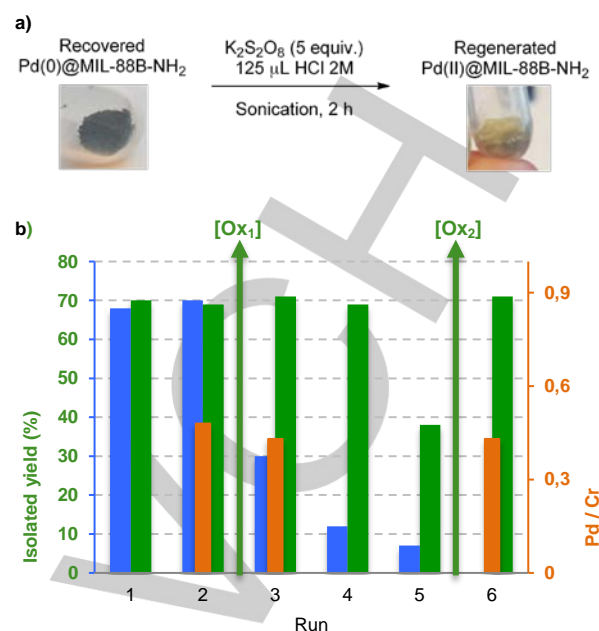
Figure 3. a) *Ex-situ* oxidative regeneration of the Pd(II)@MOF catalyst. b) New recycling experiments on a 4 mmol scale (green). Regeneration of the catalyst was performed after runs 2' and 5' (green arrows; yields obtained using the deactivated catalyst are kept in blue for easier comparison). Pd / Cr ratio in the catalyst before and after oxidative regenerations (orange) are represented in the right axis.

MIL-88B-NH$_2$ framework is preserved. This latter observation was supported by XRPD analysis, which showed a partial retention of the crystallinity after run 6' (See ESI, Figure S13).

The Pd content of the framework was analyzed by ICP-OES after runs 2', 3', and 6'. From run 2' to 3' (after Ox$_1$), a decrease of 10% in the Pd / Cr ratio was shown (Figure 3b, orange bars), although the same ratio (0.43) was retained after run 6'.

The fact that this deactivation-reactivation sequence can be repeated strengthens the hypothesis that after two reaction runs with satisfactory performance, the amount of active Pd(II) in the catalyst matrix decreases critically to form inactive Pd(0) particles.

Conclusions

A fast and green protocol for the aerobic homocoupling of arylboronic acids using a heterogeneous Pd(II)@MOF catalyst has been presented. The process was found to operate efficiently with catalytic amounts of base in aqueous EtOH (50% *v/v*) at room temperature. A wide range of substrates was tolerated, and the products were formed in good to excellent yields and isolated by simple filtration. The reaction was scaled up tenfold, and the major product was obtained in 70% yield after the same reaction time (2 h), even when the base loading was decreased. The catalyst suffered deactivation after two runs due to progressive formation of inactive Pd(0) particles. A catalyst regeneration oxidative procedure was then applied, which efficiently transformed the Pd(0) clusters into dispersed Pd(II) species, resulting in a restored catalytic activity. The regenerated catalyst displayed the same activity than the fresh one for at least two extra runs per treatment.
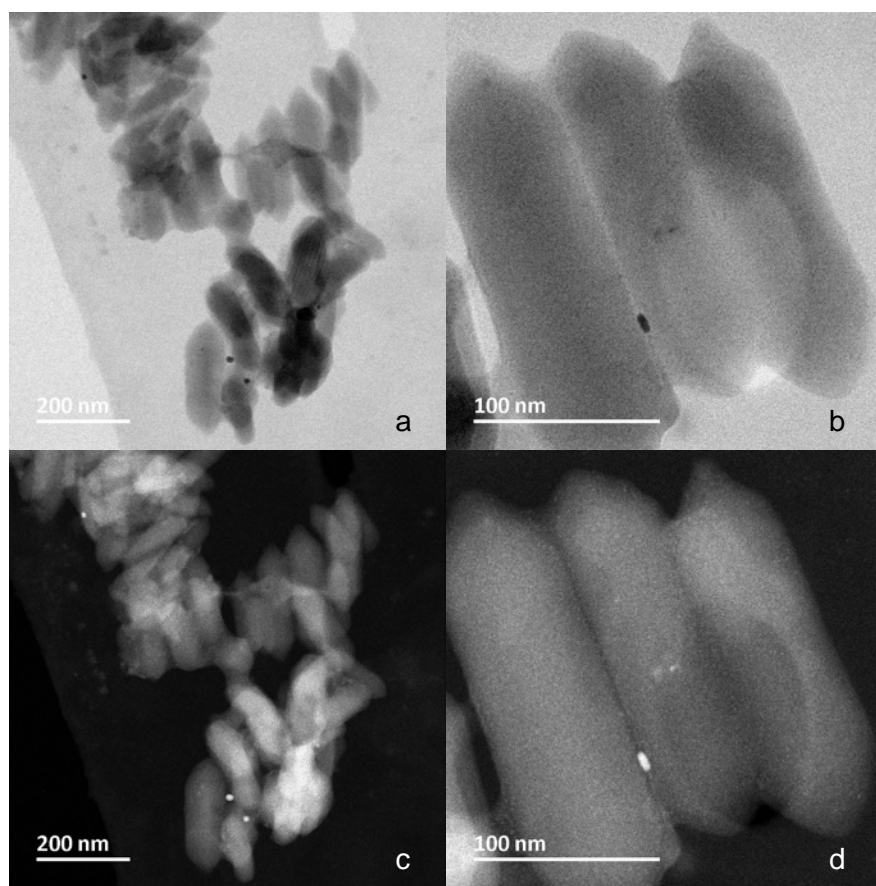
Figure 4. BF- (a, b) and HAADF-STEM (high-angle annular dark-field) images (c, d) of the Pd@MIL-88B-NH$_2$ catalyst after 5 reaction runs and the second oxidation step (Ox$_2$), prior to run 6'.

decanted. The catalyst and the precipitated product were recovered as a pellet. This solid mixture was washed and centrifuged using EtOH (2×25 mL) to dissolve and extract the product. After this procedure, the remaining clean catalyst was suspended in the reaction solvent, and the suspension was added to a new load of reagents (4 mmol scale) under an oxygen atmosphere for the next run

General procedure for the oxidative regeneration of the Pd(II)@MOF catalyst

The catalyst (0.004 mmol) recovered after run 2 was transferred to a polypropylene tube. K$_2$S$_2$O$_8$ (5.4 mg, 0.02 mmol) was added, and the solid mixture was suspended in HCl (125 μL, 2 M). A gradual lightening of the color of the starting dark green catalyst was observed. The mixture was sonicated for 2 h. After this time, the activated catalyst was suspended in the reaction solvent, and the suspension was added to a new load of reagents (4 mmol scale) under oxygen.

Experimental Section

General procedure for the homocoupling reactions

The boronic acid (2 mmol), cesium carbonate (25 mol%, 163 mg), and the Pd catalyst (2.6 mg, 9.2 wt% Pd(II)@MIL-88B-NH$_2$) were put into a round-bottomed flask (50 mL). The atmosphere was purged with oxygen (1 atm), and the flask was kept under oxygen (1 atm) using a balloon. A mixture of EtOH / H$_2$O (10 mL, v/v = 1:1) were added. When the reaction was complete, cold water (20 mL) was added, and the reaction mixture was filtered using a sintered glass funnel. The collected solid was washed with cold water (x2) to remove soluble impurities. Dichloromethane was then added to dissolve the product, and it was collected in the filtrate separated from the catalyst. This filtrate was then dried with MgSO$_4$. The solvent was evaporated under reduced pressure to give the product.

General procedure for the recycling experiments

The general procedure was followed as described. When the reaction was complete, the reaction mixture was transferred to a falcon tube. Water was added (20 mL) to promote further product precipitation and dissolution of inorganic salts. The mixture was centrifuged at low temperature (10000 rpm, 10 min, 10 °C), and the liquid phase was

[1]   a) R. A. Sheldon, J. K. Kochi in *Metal-Catalyzed Oxidations of Organic Compounds*, Academic Press, New York, **1981**; b) S. S. Stahl, *Chem. Int. Ed.* **2004**, *43*, 3400 – 3420; c) S. S. Stahl, *Science*, **2005**, *309*, 1824 – 1826; d) J. Piera, J. E. Bäckvall, *Angew. Chem. Int. Ed.* **2008**, *47*, 3506 – 3523; e) I. Funes-Ardoiz, F. Maseras, *ACS Catal.* **2018**, *8*, 1161 – 1172.

[2]   Y. Liu, G. Zhao, D. Wang, Y. Li, *Natl. Sci. Rev.* **2015**, *2*, 150 – 166.

[3]   a) Z. Zhang, T. Hashiguchi, T. Ishida, A. Hamasaki, T. Honma, H. Ohashi, T. Yokoyama, M. Tokunaga, *Org. Chem. Front.* **2015**, *2*, 654 – 660; b) S. Akbari, J. Mokhtari, Z. Mirjafari, *RSC Adv.* **2017**, *7*, 40881 – 40886.

[4]   Z. Zhang, Y. Kumamoto, T. Hashiguchi, T. Mamba, H. Murayama, E. Yamamoto, T. Ishida, T. Honma, M. Tokunaga, *ChemSusChem* **2017**, *10*, 3482 – 3489.

[5]   T. Ishida, Z. Zhang, H. Murayama, M. Tokunaga, *J. Synth. Org. Chem. Jpn.* **2017**, *75*, 1150 – 1161.

[6]   V. Sable, K. Maindan, A. R. Kapdi, P. S. Shejwalkar, K. Hara, *ACS Omega* **2017**, *2*, 204 – 217.

[7] A. de Meijere, *Handbook of Organopalladium Chemistry for Organic Synthesis,* E. Negishi, Eds., *Wiley*, New York, **2002.**

[8] K. S. Sindhu, G. Anilkumar, *RSC Adv.* **2014**, *4*, 27867 – 27887.

[9] J.M. Davidson, C. Triggs, *J. Am. Chem. Soc.* **1968**, 1324 – 1330.

[10] M. Moreno-Mañas, M. Pérez, R. Pleixats, *J. Org. Chem.* **1996**, *61*, 2346 – 2351.

[11] a) A. Lei, X. Zhang, *Tetrahedron Lett.* **2002**, *43,* 2525 – 2528; b) H. Yoshida, Y. Yamaryo, J. Ohshita, A. Kunai, *Tetrahedron Lett.* **2003**, *44*, 1541 – 1544; c) K. Cheng, B. Xin, Y. Zhang, *J. Mol. Catal. A: Chem.* **2007**, 273, 240 – 243; d) Z. Xu, J. Mao, Y. Zhang, *Catal. Commun.* **2008**, *9*, 97 – 100; e) N. Wu, X. Li, X. Xu, Y. Wang, Y. Xu, X. Chen. *Let. Org. Chem.* **2010**, *7*, 11 – 14; f) Z. Zhou, Q. Hu, Z. Du, J. Xue, S. Zhang, Y. Xie, *Synth. React. Inorg. Met. Org. Chem.* **2012**, *42*, 940 – 943; g) Z. Zhou, M. Liu, X. Wu, H. Yu, G. Xu, Y. Xie, *Appl. Organometal. Chem.* **2013**, *27*, 562 – 569; h) S. Dwivedi, S. Bardhan, P. Ghosh, S. Das, *RSC Adv.* **2014**, *4*, 41045 – 41050; i) C. A. Contreras-Celedón, J. A. Rincón-Medina, D. Mendoza-Rayo, L. Chacón-García. *Appl. Organometal. Chem.* **2015**, *29*, 439 – 442; j) J. Xia, M. Cheng, Q. Chen, M. Cai, *Appl. Organometal. Chem.* **2015**, *29*, 113 – 116; k) B. Kar, S. Bardhan, P. Ghosh, B. Ganguly, K. Kundu, S. Sarkar, B. K.Paul, S. Das, *ChemistrySelect* **2017**, *2*, 1079 – 1088.

[12] Y. Yamamoto, R. Suzuki, K. Hattori, H. Nishiyama, *Synlett* **2006**, *7*, 1027 – 1030.

[13] X. Li, D. Li, Y. Bai, C. Zhang, H. Chang, W. Gao, W. Wei, *Tetrahedron* **2016**, *72*, 6996 – 7002.

[14] a) Y. Sun, H. Zhou, *Sci. Technol. Adv. Mater.* **2015**, *16*, 054202; b) A. H. Chughtai, N. Ahmad, H. A. Younus, A. Laypkov, F. Verpoort, *Chem. Soc. Rev.* **2015**, *44*, 6804 – 6849; c) S. Yuan, L. Feng, K. Wang, J. Pang, M. Bosch, C. Lollar, Y. Sun, J. Qin, X. Yang, P. Zhang, Q. Wang, L. Zou, Y. Zhang, L. Zhang, Y. Fang, J. Li, H. Zhou, *Adv. Mater.* **2018**, 1704303; d) J. Gascon, A. Corma, F. Kapteijn, F. X. Llabres i Xamena, *ACS Catal.* **2014**, *4*, 361 – 378; e) D. Farrusseng, S. Aguado, C. Pinel, *Angew. Chem. Int. Ed.* **2009**, *48*, 7502 – 7513.

[15] a) A. Dhakshinamoorthy, A.M. Asiric, H. Garcia, *Chem. Soc. Rev.*, **2015**, *44*, 1922 – 1947. For a Perspective, see: V. Pascanu, G. González Miera, A. K. Inge, B. Martín-Matute, *J. Am. Chem. Soc., accepted for publication.*

[16] H. Furukawa, K. E. Cordova, M. O'Keeffe, O. M. Yaghi, *Science* **2013**, *341*, 1230444.

[17] a) Z. Hu, D. Zhao. *CrystEngComm.* **2017**, *19*, 4066 – 4081; b) A. Santiago-Portillo, S. Navalin, P. Concepción, M. Álvaro, H. García, *ChemCatChem* **2017**, *9*, 2506 – 2511.

[18] A. Dhakshinamoorthy, A. M. Asirib, H. Garcia, *Chem. Commun.* **2017**, *53*, 10851 – 10869.

[19] A. Dhakshinamoorthy, Z. Li, H. Garcia, *Chem. Soc. Rev.* **2018**, *47*, 8134 – 8172.

[20] a) Z. Li, A. W. Peters, A. E. Platero-Prats, J. Liu, C. Kung, H. Noh, M. R. DeStefano, N. M. Schweitzer, K. W. Chapman, J. T. Hupp, O. K. Farha, *J. Am. Chem. Soc.* **2017**, *139*, 15251 – 15258; b) Z. Li, A. W. Peters, V. Bernales, M. A. Ortuño, N. M. Schweitzer, M. R. DeStefano, L. C. Gallington, A. E. Platero-Prats, K. W. Chapman, C. J. Cramer, L. Gagliardi, J. T. Hupp, O. K. Farha, *ACS Cent. Sci.* **2017**, *3*, 31 – 38; c) C. J. Doonan, C.J. Sumby, *CrystEngComm* **2017**, *19*, 4044 – 4048.

[21] a) Q. Yang, Q. Xu, H. Jiang. *Chem. Soc. Rev.* **2017**, *46*, 4774 – 4808; b) A. Dhakshinamoorthya, H. Garcia, *Chem. Soc. Rev.*, **2012**, *41*, 5262 – 5284.

[22] a) V. Pascanu, Q. Yao, A. Bermejo Gómez, M. Gustafsson, Y. Yun, W. Wan, L. Samain, X. Zou, B. Martín-Matute, *Chem. Eur. J.* **2013**, *19*, 17483 – 17493; b) V. Pascanu, P. R. Hansen, A. Bermejo Gómez, C. Ayats, A. E. Platero-Prats, M. J. Johansson, M. À. Pericàs, B. Martín-Matute, *ChemSusChem* **2015**, *8*, 123 – 130; c) F. Carson, V. Pascanu, A. Bermejo Gómez, Y. Zhang, A. E. Platero-Prats, X. Zou, B. Martín-Matute, *Chem. Eur. J.* **2015**, *12*, 10896 – 10902.

[23] V. Pascanu, F. Carson, M. Vico Solano, J. Su, X. Zou, M. J. Johansson, B. Martín-Matute, *Chem. Eur. J.* **2016**, *22*, 3729 – 3737.

[24] A. Nagendiran, V. Pascanu, A. Bermejo Gómez, G. González Miera, C.-W. Tai, O. Verho, B. Martín-Matute, Jan-E. Bäckvall, *Chem. Eur. J.* **2016**, *22*, 7184 – 7189.

[25] N. Yuan, V. Pascanu, Z. Huang, A. Valiente, N. Heidenreich, S. Leubner, A. K. Inge, J. Gaar, N. Stock, I. Persson, B. Martin-Matute, X. Zou, *J. Am. Chem. Soc.* **2018**, *140*, 8206 – 8217.

[26] M. Vico Solano, G. González Miera, V. Pascanu, A. K. Inge, B. Martín-Matute. *ChemCatChem* **2018**, *10*, 1089 – 1095.

[27] V. Pascanu, A. Bermejo Gómez, C. Ayats, A. Platero-Prats, F. Carson, J. Su, Q. Yao, M. Pericàs, X. Zou, B. Martín-Matute, *ACS Catal.* **2015**, *5*, 472 – 479.

[28] M. Shibata, H. Ito, K. Itami, *Chem. Lett.* **2017**, *46*, 1701 – 1704.

[29] M. Ma, A. Bétard, I. Weber, N. S. Al-Hokbany, R. A. Fischer, N. Metzler-Nolte, *Cryst. Growth Des.* **2013**, *13*, 2286 – 2291.

[30] Á. Molnár. *Chem. Rev.* **2011**, *111*, 2251 – 2320.

[31] MIL-101-NH$_2$ is the mesoporous polymorph of MIL-88B-NH$_2$.

[32] Two distribution of NPs were observed: 5.2 nm and 38.0 nm average size particles co-existed.

[33] J. Chen, Q. Zhang, Y. Wang, H. Wan, *Adv. Synth. Catal.* **2008**, *350*, 453 – 464.

[34] W. C. Elias, A. M. Signori, L. Zaramello, B. L. Albuquerque, D. C. de Oliveira, J. B. Domingos, *ACS Catal.* **2017**, *7*, 1462 – 1469.

[35] K. Morgan, A. Goguet, C. Hardacre, *ACS Catal.* **2015**, *5*, 3430 – 3445.

[36] Using hypochlorite: G. V. Lowryand, M. Reinhard, *Environ. Sci. Technol.* **2000**, *34*, 3217 – 3223; Using nitric acid: Q. L. Song, S. J. Wang, B. X. Shen & J. G. Zhao, *Petrol. Sci. Technol.* **2010**, *28*, 1825 – 1833; Using permanganate: D. Angeles-Wedler, K. Mackenzie, F.-D. Kopinke, *Appl. Cat. B.* **2009**, *90*, 613 – 617.

[37] a) O.C. Feeley, W.M.H Sachtler, *Appl. Cat.* **1991**, *75*, 93 – 103; b) S.T. Homeyer, W.M.H. Sachtler, *Appl. Cat.* **1989**, *54*, 189 – 202; c) H. Birgersson, M. Boutonnet, F. Klingstedt, D.Y. Murzin, P. Stefanov, A. Naydenov, *A. Appl. Catal., B* **2006**, *65*, 93 – 100; d) P.S.Lambrou, K. Polychronopoulou, K.C. Petallidou, A.M. Efstathiou, *Catal., B* **2012**, *111*, 349 – 359.

[38] High temperature aerobic oxidation: E. J. Peterson, A. T. DeLaRiva, S. Lin, R. S. Johnson, H. Guo, J. T. Miller, J. H. Kwak, C. H. F. Peden, B. Kiefer, L. F. Allard, F. H. Ribeiro, A.K. Datye, *Nat. Commun.* **2014**, *5*, 4885.

[39] For Pd free MIL-88B-NH$_2$ see: H.-L. Wang, H. Yeh, Y.-C. Chen, Y.-C. Lai, C.-Y. Lin, K.-Y. Lu, R.-M. Ho, B.-H. Li, C.-H. Lin, D.-H. Tsai, *ACS Appl. Mater. Interfaces*, **2018**, *10*, 9332 – 9341.

Entry for the Table of Contents

FULL PAPER

Palladium(II) supported on the metal-organic framework MIL-88B-NH$_2$ is an excellent catalyst for the aerobic homocoupling of arylboronic acids. A detailed study of how the activity of the catalyst can be restored without compromising its efficiency is presented.
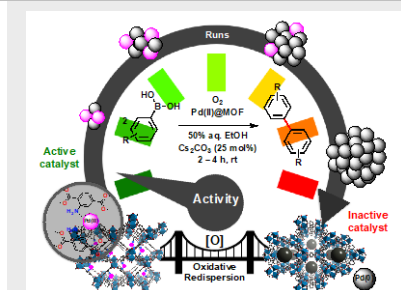
Alejandro Valiente, Sergio Carrasco, Amparo Sanz-Ma... Cheuk-Wai Tai, Antonio Bermejo Gómez, and Belén M... Matute*

Page No. – Page No.

Aerobic Homocoupling of Arylboronic Acids Catal... Regenerable Pd(II)@MIL-88B-NH$_2$(Cr)